RESEARCH ARTICLE

# 3D-printed Bioresorbable Stent Coated with Dipyridamole-Loaded Nanofiber for Restenosis Prevention and Endothelialization

**Chengjin Wang[1,2,3], Yang Yang[1,2,3], Jingyuan Ji[1,2,3], Yongcong Fang[1,2], Liliang Ouyang[1,2,3], Lei Zhang[1,2,3]*, Wei Sun[1,2,3,4]***

[1]Biomanufacturing Center, Department of Mechanical Engineering, Tsinghua University, Beijing 100084, China
[2]Biomanufacturing and Rapid Forming Technology Key Laboratory of Beijing, Beijing 100084, China
[3]"Biomanufacturing and Engineering Living Systems" Innovation International Talents Base (111 Base), Beijing 100084, China
[4]Department of Mechanical Engineering, Drexel University, Philadelphia, PA 19104, USA

**Abstract:** Intimal hyperplasia and restenosis caused by excessive proliferation of smooth muscle cells (SMC) are the main factors for the failure of stent implantation. Drug-eluting stents carried with antiproliferative drugs have emerged as a successful approach to alleviate early neointimal development. However, these agents have been reported to have an undesirable effect on re-endothelialization. In this study, we proposed an integrated bioresorbable stent coated with dipyridamole (DP)-loaded poly(D,L-lactide) (PDLLA) nanofibers. Three-dimensional (3D) bioresorbable stents were fabricated by printing on a rotation mandrel using polycaprolactone (PCL), and the stents were further coated with PDLLA/DP nanofibers. The in vitro degradation and drug release evaluation illustrated the potential for long-term release of DP. Stents coated with PDLLA/DP nanofibers showed excellent hemocompatibility. The cell viability, proliferation, and morphology analysis results revealed that stents coated with PDLLA/DP nanofibers could prevent the proliferation of SMC and have no adverse effects on endothelial cells. The in vivo implantation of stents coated with PDLLA/DP nanofibers showed initial patency and continuous endothelialization and alleviated neointimal formation. The attractive in vitro and in vivo performance indicated its potential for restenosis prevention and endothelialization.

**Keywords:** Bioresorbable stent; Nanofiber; Dipyridamole; Anti-restenosis; Endothelialization

*Correspondence to: Lei Zhang, Biomanufacturing Center, Department of Mechanical Engineering, Tsinghua University, Beijing 100084, China; stoneszhang@mail.tsinghua.edu.cn; Wei Sun, Biomanufacturing Center, Department of Mechanical Engineering, Tsinghua University, Beijing 100084, China; weisun@mail.tsinghua.edu.cn

**Received:** January 13, 2022; **Accepted:** February 19, 2022; **Published Online:** February 19, 2022

(This article belongs to the *Special Issue: Composite/Multi-component Biomaterial Inks and Bioinks*)

**Citation**: Wang, C., Yang, Y., Ji, J., *et al*., 2022, 3D-Printed Bioresorbable Stent Coated with Dipyridamole-Loaded Nanofiber for Restenosis Prevention and Endothelialization. *Int J Bioprint,* 8(2):543. http://doi.org/10.18063/ijb.v8i2.543

## 1. Introduction

In recent years, metallic drug-eluting stents (DES) have become an effective clinical treatment for coronary artery disease, which work by introducing antiproliferative drug-loaded polymer coatings that can inhibit smooth muscle cell (SMC) proliferation and alleviate neointimal development[1,2]. However, residual metallic stents as foreign objects would cage the vessel permanently, leading to late stent thrombosis, impaired coronary vasomotion, and prolonged dual antiplatelet therapy[3,4]. Moreover, antiproliferative agents loaded in the polymer coating of DES, such as sirolimus and paclitaxel, have been reported to have an undesirable effect on re-endothelialization, which may result in long-term endothelial dysfunction[5,6].

To overcome the inherent drawbacks of permanently existing metallic stents, bioresorbable stents have been developed to provide temporary support with tunable degradation rates of stent materials[7]. Bioresorbable

stents have been demonstrated to facilitate the recovery of vasomotion and reduce the risk of late thrombosis[8,9]. Laser cutting is the conventional manufacturing technique for metal stents and bioresorbable polymeric stents. However, laser processing as a thermal process will cause heat-affected zones and microcracks and reduce a stent's fatigue life, especially for polymeric stents[10]. In our previous study[11], we developed a custom-made four-axis three-dimensional (3D) printing system with a novel mini-screw extruder and a rotation mandrel to realize precise extrusion of polymer filaments. We successfully developed a novel stent with a zero Poisson's ratio structure to address the longitudinal foreshortening problem of conventional metal stents. Moreover, bioresorbable polycaprolactone (PCL) stents with adjustable stent structures and shapes were fabricated by 3D printing.

To alleviate the limitations of antiproliferative agents on endothelialization, drugs that could impede SMC proliferation and have no detrimental effect on endothelial cell viability have been explored as coatings for vascular stents. Dipyridamole (DP), an antithrombotic and antithrombogenic drug used in the clinic, can impede the proliferation of SMCs by hindering the uptake of adenosine[12]. More importantly, DP has been reported to facilitate the proliferation and endothelialization of vascular endothelial cells[13]. Therefore, it is reasonable to develop a biodegradable polymer coating with the combination of versatile DP to address the dilemma of current antiproliferative agent-loaded DES. Various approaches, including dip coating[14], spray coating[15,16], and electrospinning[17], have been explored to achieve polymer/drug coating with stents. Among them, electrospinning has been reported to be a versatile and economical technology to produce nanofibers for biomedical applications[18]. Compared to DES, stents coated with drug-loaded nanofibers might introduce additional benefits. For example, drug-loaded nanofibers mimic the microenvironment of the native extracellular matrix and provide a high surface-to-volume ratio, which is beneficial for cell adhesion and proliferation, more uniform drug release, and higher doses of agents[19]. In addition, it is flexible to select different polymers as the carrier of agents[20]. Punnakitikashem *et al*.[21] reported a biodegradable vascular graft with nanofibrous structures electrospun by mixing polyurethane with DP, achieving sustained release of DP for more than 91 days. Liu *et al*.[22] fabricated bare-metal stents coated with poly(l-lactide-co-caprolactone) nanofibers loaded with both heparin and rosuvastatin using coaxial electrospinning for the treatment of aneurysms. This study demonstrated that nanofibers with shell-core structures could load different drugs with adjustable ratios and spatial distribution, suggesting the flexibility and compatibility of electrospun nanofibers for drug release. The release rate and drug loading capacity could be easily tuned by using various combinations of polymer nanofibers and structural designs.

Despite the progress of metal stents coated with drug-loaded nanofibers, the performance of drug-loaded nanofibers based on bioresorbable stents has not been well investigated. Accordingly, to overcome the challenges associated with DES, such as permanent metallic stents and the limitations of antiproliferative agents on endothelialization, we propose a strategy to combine bioresorbable stents with DP-loaded nanofiber coatings that could prevent in-stent restenosis and promote neo-endothelialization. As depicted in **Figure 1**, we developed an integrated stent with the combination of biodegradable polymers as the backbone material of 3D-printed stents and DP-loaded nanofibers as the coating. 3D bioresorbable stents were fabricated by printing on a rotation mandrel using PCL, and the stents were further coated with DP-loaded poly(D,L-lactide) (PDLLA) nanofibers by electrospinning. The surface morphology and radial strength of the stents were characterized by scanning electron microscopy (SEM) and radial compression tests, respectively. The in vitro drug release, degradation, and Fourier transform infrared (FTIR) characterization of PDLLA/DP nanofibers were investigated and a long-term sustained release of DP drug over 120 days was achieved. In addition, the in vitro hemocompatibility and biocompatibility results suggested that stents coated with DP-loaded nanofibers significantly inhibited the proliferation of SMCs and facilitated the endothelializtion of vascular endothelial cells. Moreover, in vivo evaluation of stent implantation was carried out using a porcine coronary artery model. After implantation for 28 days, the arteries implanted with DP-loaded stents showed reduced in-stent restenosis and initial endothelialization.

## 2. Materials and methods

### 2.1. Materials

PCL (average Mn 80000) and DP were purchased from Sigma-Aldrich (St. Louis, USA). 1,1,1,3,3,3-hexafluoro-2-propanol (HFIP, 99+%) was supplied by Aladdin Co., Ltd. (Shanghai, China). PDLLA (Mn = 10 kDa) was purchased from Jinan Daigang Biomaterial Co., Ltd. (Jinan, China).

### 2.2. 3D-printed PCL stents coated with PDLLA/DP nanofibers

A custom-made four-axis 3D printing system with a novel mini-screw extruder and a rotation mandrel reported in our previous study was applied to fabricate tubular PCL stents[11]. As illustrated in **Figure 1A(i)**, the PCL material was molten and extruded through the nozzle into filaments and further deposited on the rotating mandrel. Stents with an inner diameter of 3 mm and a length of 10 mm were fabricated. Subsequently, as illustrated in **Figure 1A(ii)**, PDLLA nanofibers loaded with DP were randomly deposited onto

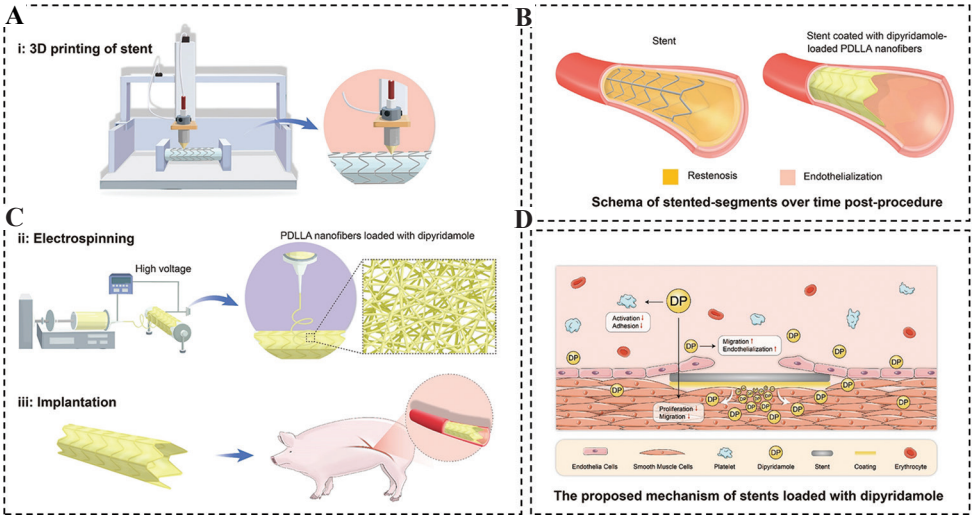


**Figure 1.** Fabrication of a 3D-printed bioresorbable stent coated with dipyridamole (DP)-loaded nanofiber and its mechanism for restenosis prevention and endothelialization. (A) Fabrication and implantation of stents coated with DP-loaded dipyridamole-loaded poly(D,L-lactide) (PDLLA) nanofibers, (i) 3D-printed stents were prepared using a 3D printing system with a rotation mandrel, (ii) PDLLA nanofibers loaded with DP were randomly deposited onto 3D-printed stents, and (iii) stents were implanted into porcine coronary arteries for in vivo evaluation. (B) The artery segment implanted with the bare stent exhibited more severe in-stent restenosis, while the artery implanted with DP-loaded stents showed initial endothelialization. (C) The proposed mechanism of stents coated with DP-loaded nanofibers for antiplatelet adhesion, the inhibition of smooth muscle cells proliferation, and enhanced endothelial cell growth.

3D-printed PCL stents. A similar electrospinning process was introduced in our previous work[23]. With the rotation of the mandrel, PDLLA/DP nanofibers were uniformly deposited onto 3D-printed stents. Thus, 3D-printed PCL stents coated with PDLLA/DP nanofibers were accomplished. To further demonstrate the function of PDLLA/DP nanofibers, bare stents and stents coated with only PDLLA nanofibers (without DP) were prepared as control groups.

## 2.3. Morphological and mechanical characterization of stents

The surface morphology of 3D-printed PCL stents, stents coated with only PDLLA nanofibers, and stents coated with PDLLA/DP nanofibers was characterized by SEM (ZEISS GeminiSEM 300, Germany). To further observe the morphology of the inside view of stents, stents were cut in half from the middle before SEM characterization. In this study, the crush resistance test using parallel plates was conducted by a mechanical test instrument (BOSE 3230, Germany). The stents used in this test possessed an inner diameter of 3 mm and a length of 10 mm. The stent was placed between two plates and compressed to a displacement of 1.5 mm (half of the stent inner diameter) at a constant moving speed of 1 mm/min. For each group, three samples were used to record the "Force-Displacement" curve.

## 2.4. Morphological and FTIR characterization of electrospun nanofibers

The morphology of PDLLA and PDLLA/DP nanofibers was obtained by SEM observation. The chemical bonding of DP, PDLLA nanofibers, and PDLLA/DP nanofibers was examined by FTIR spectroscopy (Bruker V70, Germany). The scanning wavenumber range was from 4000 $cm^{-1}$ to 600 $cm^{-1}$.

## 2.5. Electrical conductivity

The electrical conductivity of different polymer solutions was measured using a conductometer (DDS-11A, INESA Scientific Instrument Co., Ltd., Shanghai, China). 5 mL of each polymer solution was measured at 25°C. Three samples (n = 3) from each group were used.

## 2.6. In vitro drug release and degradation

To investigate the in vitro drug release behavior of DP from PDLLA/DP nanofibers, weighted electrospun nanofiber mats were immersed in 10 ml of phosphate-buffered saline (PBS, pH 7.4). The samples (n = 6) were incubated at 37°C. At predefined time points, 10 mL of PBS solution with the released drug was collected, and 10 mL of fresh PBS was replenished. The absorbance value of PBS with released DP was recorded at 284 nm by an ultraviolet-visible spectrophotometer (HITACHI U3900, Japan). To plot the standard curve of DP concentration versus absorbance in PBS, the absorbance of different solutions with concentrations from 1 μg/mL to 100 μg/mL was measured. To obtain the whole drug release result, the absorbance value was accumulated based on the previous values.

To determine the in vitro degradation behavior, PDLLA/DP nanofibers were immersed in PBS, and

then samples were kept at 37°C. PBS was replaced at weekly intervals. At predefined time points, samples were weighed to record the residual mass after rinsing and vacuum drying. SEM observation of nanofibers after degradation was performed to analyze fiber morphology and integrity. Three replicates of each group were used at each time point.

## 2.7. In vitro hemocompatibility evaluation

In this study, the in vitro hemocompatibility evaluation was performed following the International Standard (ISO 10993-4) and National Standard of the People's Republic of China (GB/T 16886.4). To evaluate the hemocompatibility of different stents, male Sprague-Dawley rats (8 weeks old) were applied to obtain fresh whole blood.

### *(1) Platelet adhesion*

To collect platelet-rich plasma (PRP), fresh whole blood was centrifuged at 1500 rpm for 10 min. As a previous study reported[24], 3D-printed bare PCL stents, stents coated with PDLLA nanofibers, and stents coated with PDLLA/DP nanofibers were incubated in PRP for 30 min at 37°C and washed 3 times in PBS. The samples were fixed, dehydrated, air-dried in sequence, and then observed by SEM.

### *(2) Hemolysis analysis*

As reported in the previous studies[24,25], the hemolysis rate was measured by detecting hemoglobin release. Briefly, 3D-printed bare PCL stents, stents coated with PDLLA nanofibers, and stents coated with PDLLA/DP nanofibers were soaked in 10 mL of normal saline at 37°C for 60 min. Fresh whole blood (4 mL) was diluted by adding 5 mL of normal saline, and then 0.2 mL of diluted blood was added to these centrifuge tubes. Similarly, 10 mL of deionized water and normal saline solution were set as positive and negative controls, respectively. After incubation at 37°C for 60 min, all samples were centrifuged for 5 min at 3000 rpm to collect the supernatant. The optical density (OD) of the supernatant was recorded at 545 nm by a spectrophotometer (NanoDrop 2000, Thermo, USA).

## 2.8. In vitro biocompatibility assessment

In this study, rat aortic SMC (RASMCs) were purchased from Shanghai Zhong Qiao Xin Zhou Biotechnology Co., Ltd. (Shanghai, China), and human umbilical vein endothelial cells (HUVECs) were obtained from American Type Culture Collection (ATCC, USA). RASMCs were cultured in Dulbecco's modified eagle medium (DMEM) supplemented with 10% fetal bovine serum and 1% penicillin-streptomycin. HUVECs were cultured in endothelial cell growth medium-2 (EGM-2, Lonza, Switzerland).

### *(1) Cytotoxicity analysis*

To collect the extracts of different groups, bare PCL stents, stents coated with PDLLA nanofibers, and stents coated with PDLLA/DP nanofibers were immersed in a culture medium of RASMCs and HUVECs at 37°C for 24 h, respectively. The cell suspensions of RASMCs and HUVECs were added to 96-well plates at densities of $5.0 \times 10^3$/100 μL in each well. The plates were incubated at 37°C with 5% $CO_2$. After 24 h of incubation, the cell culture medium was replaced by extracts of different groups. After culturing in extracts for 48 h, 10 μL of cell counting kit-8 (CCK-8, Dojindo Laboratories, Japan) per 100 μL of culture medium was slowly instilled into each well, and then the plates were incubated for 3 h at 37°C with 5% $CO_2$. Subsequently, the absorbance value for each well was recorded at 450 nm using a microplate reader (Multiskan, Thermo, USA). Cell viability was calculated in detail elsewhere[11].

### *(2) Cell viability and proliferation*

RASMCs and HUVECs were seeded in different stents to assess biocompatibility via cell viability and proliferation experiments, respectively. Before seeding the cells, the specimens were sterilized in 75% ethanol for 5 h, washed 3 times in PBS, irradiated with UV for 1 h, and then incubated in culture medium overnight. Stents were transferred into a new 24-well plate, and then RASMCs and HUVECs were seeded onto the inside surface of stents at densities of $5.0 \times 10^4$ and $1.0 \times 10^5$ cells per well, respectively. All samples were incubated at 37°C with 5% $CO_2$. The cell culture medium was changed every 2 days. For cell-seeded stents, cell viability was analyzed by a cell live/dead staining assay kit (Dojindo, Japan) on days 1 and 7, according to the manufacturer's instructions. Samples were observed using a laser confocal microscope (Nikon A1, Japan). In addition, CCK-8 was applied to evaluate cell proliferation on days 1, 4, and 7.

### *(3) Cell morphological analysis*

To further observe the cell morphology of the RASMCs and HUVECs on different stents, cytoskeletal staining and SEM analysis were conducted after culture for 7 days. Samples for immunostaining and SEM observation were treated with the same process as reported in our previous work[23].

## 2.9. In vivo evaluation of stent implantation

Six healthy white minipigs weighing 30 ± 5 kg were used in this study. All experimental procedures were carried out with approval by the Animal Ethics Committee of Nongnong Life Science and Technology Company (Beijing, China). 3D-printed bare PCL stents and stents coated with PDLLA/DP nanofibers (inner diameter:

3 mm, length: 15 mm) were prepared and sterilized using 15 kGy of gamma radiation before implantation. Six white minipigs were divided into two groups (group one and group two). Stents coated with PDLLA/DP nanofibers (n = 3) were implanted into group one, while PCL bare stents (n = 3) were implanted into group two as the control group.

Stents were positioned into the coronary arteries of pigs. Balloons with crimped stents were dilated with 10 atm for 30 s to realize a stent-to-artery diameter ratio of 1.2:1. Coronary angiography was recorded after implantation for days 1 and 28. After stents were implanted for 28 days, pigs were euthanized to harvest the stented artery samples. Then, samples were fixed in 10% formalin for 24 h, dehydrated and embedded in paraffin for cross-section slicing. Hematoxylin and eosin (H&E) and Masson staining were performed for histological analysis.

### 2.10. Statistical analysis

Experimental data are presented as the mean ± standard deviation (SD). The statistical analysis software GraphPad Prism 8.0 was used for Student's *t*-test.

## 3. Results

### 3.1. Fabrication and characterization of PDLLA/DP nanofibers

The diameter of electrospun fibers typically ranges from tens of nanometers to several micrometers[26]. The morphology of electrospun fibers was influenced by the polymer solution composition and processing parameters. We first optimized the electrospinning process with the base polymer PDLLA. The morphology of PDLLA nanofibers was investigated using different concentrations of PDLLA/HFIP solutions (100, 150, 200, and 250 mg/mL) and flow rates (0.5, 1.0, and 2.0 mL/h). As shown in **Figure S1**, in general, PDLLA fibers became more uniform with the increase of PDLLA concentration. The formation of beads was observed and gradually became unapparent at concentrations of 100, 150, and 200 mg/mL, while uniform nanofibers with smooth surfaces were achieved at concentrations of 250 mg/mL (**Figure S1A**). Fong *et al*.[27] reported that a higher viscosity of polymer solutions could facilitate the formation of fibers without beads, which was confirmed by our results. Thus, the PDLLA/HFIP polymer solution concentration was set as 250 mg/mL in the present work. The effect of the flow rate of polymer solution on the nanofiber morphology was further evaluated. As presented in **Figure S1B**, there was no obvious difference in the morphology of PDLLA fibers prepared with flow rates of 0.5, 1.0, and 2.0 mL/h. To achieve a more compact structure, we selected a higher flow rate (2.0 mL/h) in the following studies.

Electrospun fibers loaded with DP have been reported to realize sustained release for up to weeks. Punnakitikashem *et al*.[21] developed a nanofibrous scaffold with a higher DP content (10%), which inhibited SMC proliferation and showed no adverse effect on endothelial cells. A similar concentration of DP in the solution was also used to prepare drug-loaded nanofibers to achieve the antiplatelet effect[28,29]. Here, DP was dissolved in PDLLA/HFIP solution at a concentration of 10% to PDLLA. Thus, the concentration of DP in polymer solution was 25 mg/mL. PDLLA/DP nanofibers with an average diameter of 247.01 ± 44.65 nm showed a relatively uniform morphology and compact diameter distribution, as shown in **Figure 2A(i)**. In contrast, plain PDLLA nanofibers exhibited an average diameter of 685.54 ± 252.23 nm and possessed a bimodal distribution of fiber diameter, as depicted in **Figure S1C**.

Subsequently, FTIR characterization was performed to investigate the chemical structure of DP, PDLLA nanofibers, and PDLLA/DP nanofibers. Since the concentration of DP in the mixture of PDLLA/DP was only 10%, these peaks with low absorbance in the FTIR spectra of DP were not obvious in the spectra of PDLLA/DP. Therefore, we mainly focused on the characteristic peaks in each spectrum. As shown in **Figure 2B**, the most obvious peak in the spectra of DP was detected at 1527 $cm^{-1}$, which was correlated to C=N bonding and absent in the spectra of PDLLA. Similarly, peaks at approximately 1750 $cm^{-1}$ (C=O), 1185 $cm^{-1}$, and 1085 $cm^{-1}$ (C-O-C) were detected in the spectra of PDLLA but absent in the spectra of DP. After the loading of DP into PDLLA fibers, all peaks that were obvious in the spectra of DP or PDLLA were retained in the spectra of PDLLA/DP. These results indicated that the PDLLA/DP nanofibers maintained their chemical stability.

The morphologies of PDLLA/DP fibers at different degradation times were investigated. As presented in **Figure 2A(i)**, fibers possessed a uniform and centralized diameter distribution (247.01 ± 44.65 nm) before degradation (0 week). After degradation for 8 weeks, the diameter of the fibers slightly decreased (234.73 ± 80.48 nm), and the diameter distribution of the PDLLA/DP fibers flattened (**Figure 2A(ii)**). When the degradation lasted for 16 weeks, the diameter of the PDLLA/DP fibers showed an obvious decrease to 145.70 ± 66.87 nm compared to that after 8 weeks of degradation (**Figure 2D**). In addition, broken fibers were observed due to accelerated degradation (**Figure 2A(iii)**). Furthermore, the representative release curve of DP from PDLLA/DP nanofibers is presented in **Figure 2C**, which shows sustained and long-term drug release. In the initial 7 days, the release maintained a relatively fast rate, especially in the first 24 h. The release rate gradually stabilized in the following days. Approximately 60% of

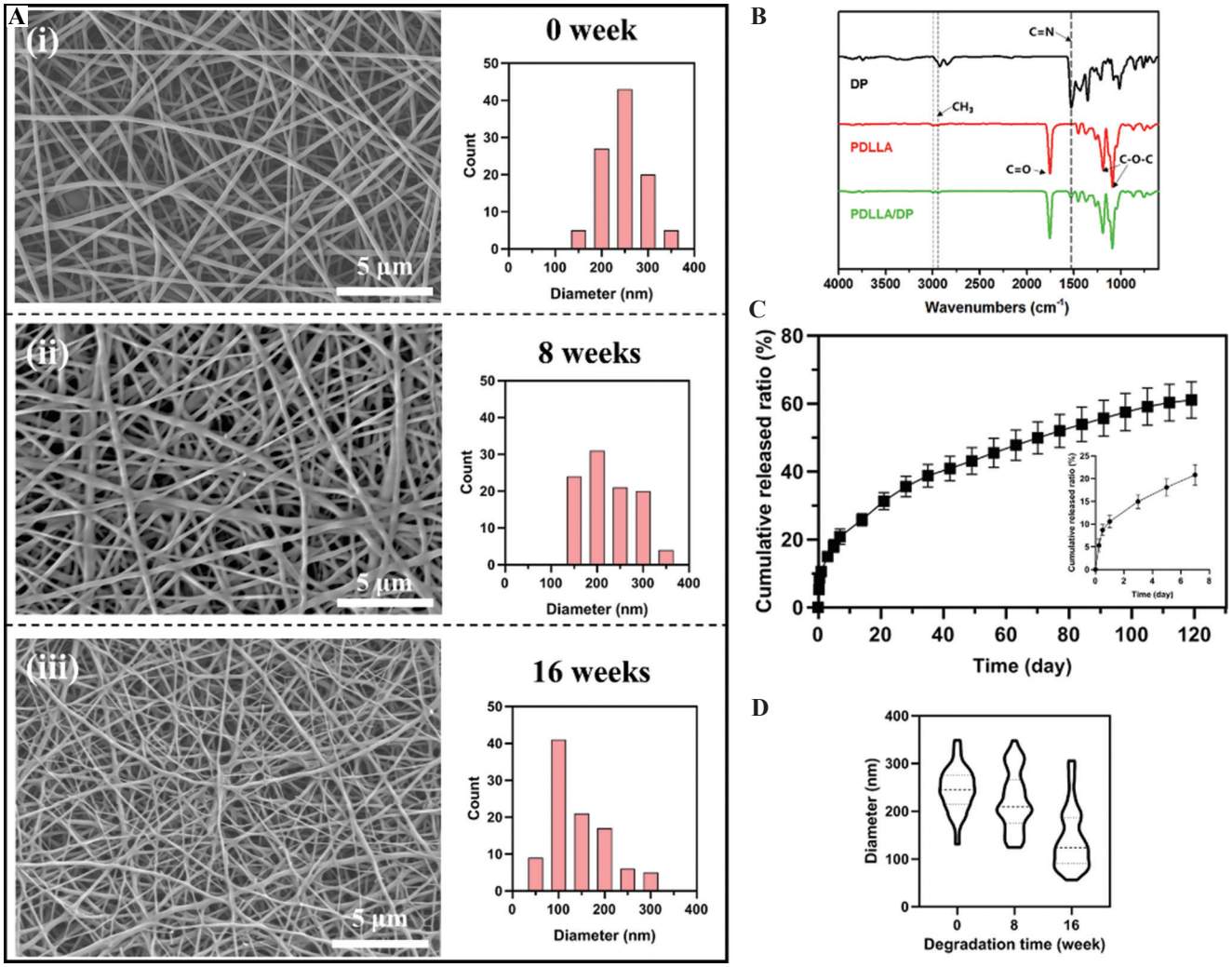


**Figure 2.** Morphology, drug release, and degradation of dipyridamole-loaded poly(D,L-lactide) (PDLLA)/DP nanofibers. (A) Scanning electron microscopy (SEM) images and distribution of fiber diameter of PDLLA/DP nanofibers before degradation at different degradation times: (i): 0 week, (ii) 8 weeks, and (iii) 16 weeks. (B) Fourier transform infrared spectra of DP, PDLLA nanofibers, and PDLLA/DP nanofibers. (C) In vitro DP release curve showed long-term drug release up to 120 days. (D) The average fiber diameters of PDLLA/DP nanofibers at different degradation times. Six samples (n = 6) from each group were used in the drug release test. The average diameters of PDLLA/DP nanofibers at different degradation times were obtained from 100 measurements using three SEM images for each time point.

DP was released during the 120-day long-term sustained release.

### 3.2. Fabrication and characterization of 3D-printed PCL stents coated with PDLLA/DP nanofibers

3D printing has emerged as a desirable technology for personalized customization and medical applications. To realize the development of customizable bioresorbable stents, we developed a four-axis 3D printing system with a novel mini-screw extruder and a rotation mandrel and fabricated 3D-printed PCL stents. The 3D model, 3D-printing trajectory strategy, and fabrication process of 3D-printed stents are presented in **Figure 3A** and **3B**. The surface morphologies of the stents with different magnifications and views are shown in **Figure 3C-E** (inside view) and **Figure S3** (outside view). Both the outside and inside surfaces of the stents showed smooth morphology. Furthermore, PDLLA/DP nanofibers prepared by the electrospinning technique were deposited onto 3D-printed PCL stents. For the control group, stents coated with PDLLA nanofibers were fabricated. SEM images of stents coated with PDLLA or PDLLA/DP nanofibers are illustrated in **Figure 3** and **Figure S3**. To better differentiate the three types of stents, the bare 3D-printed bare PCL stent, stent coated with PDLLA nanofibers, and stent coated with PDLLA/DP nanofibers were depicted as the "Stent" group, "Stent + Nano-PDLLA" group, and "Stent + Nano-PDLLA-DP" group,

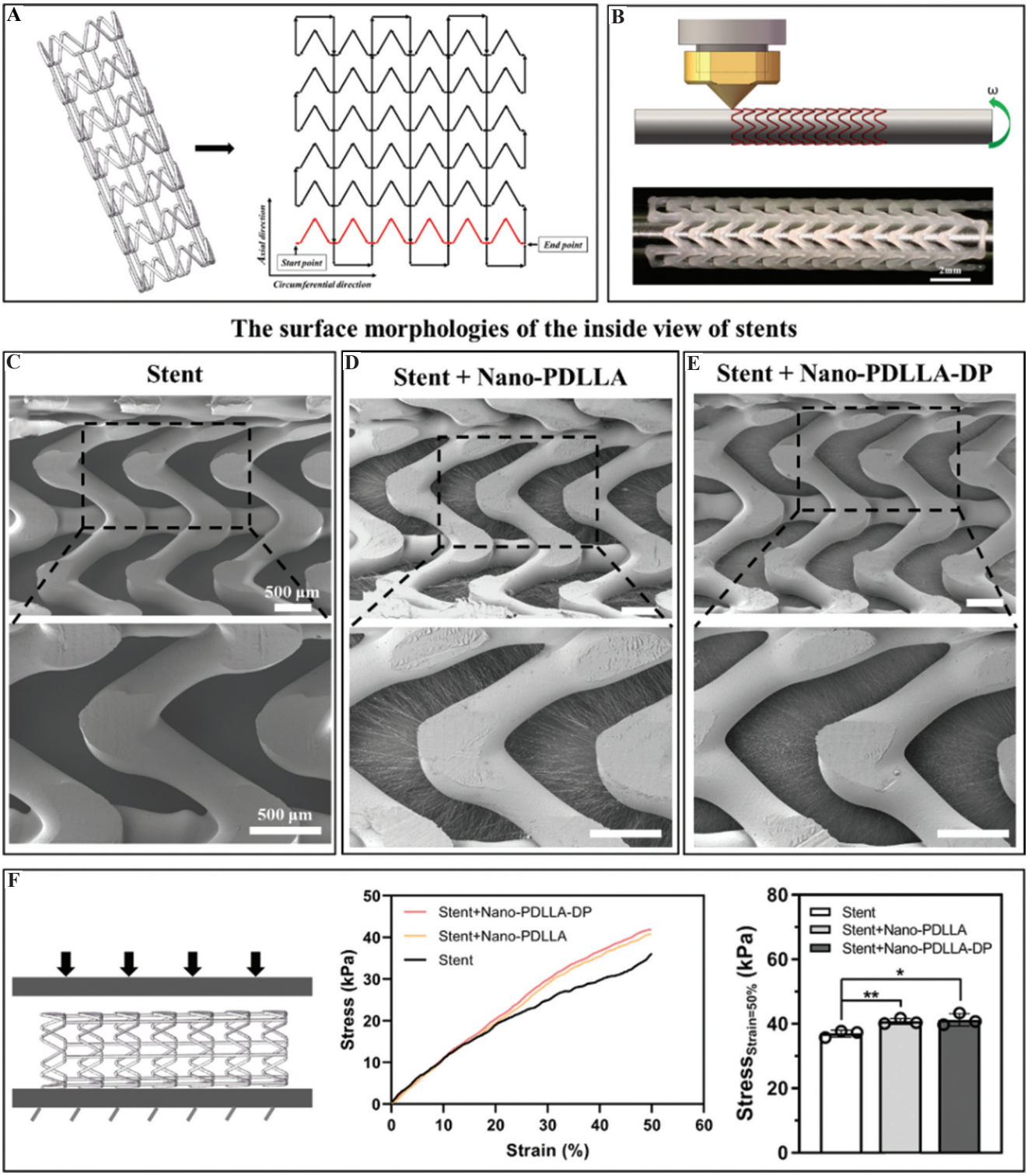


**Figure 3.** Fabrication and characterization of different stents. (A) 3D-printing trajectory strategy. (B) Schematic of the stent fabrication process. (C-E) The surface morphologies of the inside view of stents, (C) 3D-printed polycaprolactone stents, (D) stents coated with dipyridamole-loaded poly(D,L-lactide) (PDLLA) nanofibers, and (E) stents coated with PDLLA/DP nanofibers. (F) The radial compression test of different stents. Three samples (n = 3) from each group were used in the radial compression test. *$P < 0.05$, **$P < 0.01$.

respectively. In accordance with the results of electrospun fibers in **Figure 2** and **Figure S1**, PDLLA/DP fibers possessed a more compact structure and relatively uniform morphology compared to PDLLA fibers.

The radial crush resistance property is an essential indicator to respond the ability of stents to resist radial deformation. A parallel plate compression test was accomplished to record the load and displacement in the compression process. Stents with a length of 10 mm and a diameter of 3 mm were applied in this test. Stents were compressed until a radical deformation of 1.5 mm, and the load and displacement were continuously recorded in this process. As presented in **Figure 3F**, the stress–strain behavior suggested that the radial strength of stents with added nanofibers was slightly enhanced compared to that of the bare stent group. There was no significant difference between the "Stent + Nano-PDLLA" group and the "Stent + Nano-PDLLA-DP" group. The quantitative analysis of the stress value when the strain was 50% further corroborated the above results.

## 3.3. In vitro hemocompatibility evaluation

Thrombosis caused by platelet adhesion is a complication of stent implantation[30]. Thus, it is necessary to assess the hemocompatibility of stents. The platelet adhesion test was accomplished in the current study to evaluate the hemocompatibility of vascular implants. The surface morphology of adhered platelets on different stents is presented in **Figure 4A**. The red circles indicate the positions of adhered platelets, and the area of the red circles is proportional to the number of platelets inside. Compared to the bare PCL stents, stents coated with PDLLA nanofibers showed extensively increased platelet adhesion. Remarkably, compared with the "Stent + Nano-PDLLA" group, the number of adherent platelets in the "Stent + Nano-PDLLA-DP" group was significantly reduced due to the addition of DP agents.

Moreover, a hemolysis test can indicate whether samples destroy the structure of erythrocytes. As presented in **Figure 4B**, the hemolysis ratios of the three groups were less than the safe value (5%). In particular, the "Stent + Nano-PDLLA-DP" group could intensively reduce the hemolysis ratio to 1.00 ± 0.42%, compared with the hemolysis ratio of 2.91 ± 0.44% for the bare PCL stents, and 2.76 ± 0.41% for the stents coated with PDLLA nanofibers.

## 3.4. In vitro biocompatibility assessment

Here, RASMCs and HUVECs were selected to investigate the biocompatibility of stents. In particular, we investigated the effect of DP agents released from stents on cytotoxicity, cell viability and proliferation, and cell morphology.

### *(1)* In vitro *cytotoxicity testing*

Cytotoxicity is an essential biological indicator in the toxicity evaluation of medical devices[31]. According to ISO 10993- 5:2009[32], the extract test method was applied to determine the in vitro cytotoxicity of stents. According to the value of relative cell viability, the cytotoxicity of the medical devices or materials was graded as none (>100%), slight (80 – 99%), mild (50 – 79%), moderate (30 – 49%), and severe (0 – 29%). Samples were considered to have cytotoxic effects, as relative cell viability was <80%. As depicted in **Figure S5**, the cell viability of RASMCs cultured in the extract of the "Stent + Nano-PDLLA-DP" group (48.92 ± 2.05%) showed a significant decrease, compared to the "Stent" group (96.14 ± 6.21%) and "Stent + Nano-PDLLA" group (90.40 ± 3.86%). In contrast, there was no significant difference in the cell viability of HUVECs among the three groups (all >90%), and all specimens showed no obvious cytotoxic function.

### *(2) Cell proliferation and morphology analysis of RASMCs seeded on stents*

To further demonstrate the cell morphology of RASMCs and HUVECs on different stents, cytoskeletal immunofluorescence staining and SEM observation were carried out. Fluorescent phalloidin was used to bind to F-actin, which is a key cytoskeletal component and could help to identify the overall shape and structure of the cell. However, because of the opaque characteristic of the PCL thick fibers of stents, only cells attached between adjacent V-shaped struts could be observed in immunofluorescence staining images. Thus, SEM characterization was accomplished to show the overall distribution of cells.

As shown in **Figure 5A** and **5B**, RASMCs seeded on the "Stent + Nano-PDLLA" group showed a significantly higher cell proliferation rate than those seeded on the bare stent group. Compared to the "Stent + Nano-PDLLA" group, the "Stent + Nano-PDLLA-DP" group showed significantly decreased cell proliferation. In addition, the proliferation of RASMCs on day 7 showed no significant difference between the bare stents and stents with PDLLA/DP nanofibers. As shown in **Figure 5C** and **5D**, the surface of bare PCL stents and stents coated with PDLLA nanofibers was sufficiently covered with RASMCs after culture for 7 days. In the bare PCL stent group (**Figure 5C(i)** and **5D(i)**), RASMCs were only closely deposited on the surface of the PCL struts and exhibited powerful proliferation ability, despite the limited contact area and microenvironment. Remarkably, RASMCs crazily overspread the surface of stents coated with PDLLA nanofibers (**Figure 5C(ii)** and **5D(ii)**). As depicted in **Figure 5C(iii)** and 5D**(iii)**, the proliferation of RASMCs in the "Stent + Nano-PDLLA-DP" group was significantly suppressed compared with that of stents coated with only PDLLA nanofibers. It is worth mentioning that DP is a pyrimidine derivative and has a similar structure to thymine (one of the four constituent bases of nucleic acids), leading to the reaction between DAPI and DP. Thus, the cell nuclei of cells seeded in the "Stent + Nano-PDLLA-DP" group were absent in the

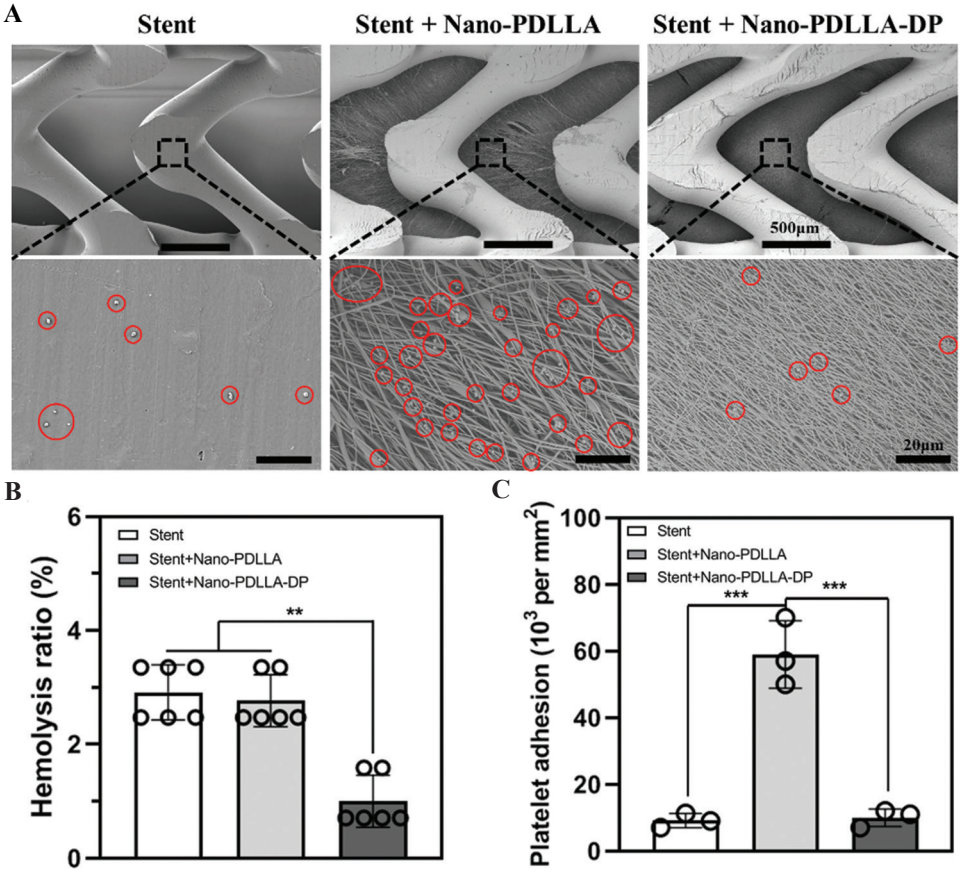


**Figure 4.** In vitro hemocompatibility evaluation of stents with different structures and compositions. (A) Scanning electron microscopy images of adhered platelets on different stents, and the red circles indicate the positions of adhered platelets. (B) Hemolysis ratios of different stents. (C) The number of adherent platelets on different stents. Six samples (n = 6) from each group were used in the hemolysis evaluation. Three samples (n = 3) of each group were used in the platelet adhesion test. $^{**}P < 0.01$. $^{***}P < 0.001$.

immunofluorescence staining images (**Figure 5C(iii)** and **6C(iii)**), due to the rapid combination of DAPI and DP.

### *(3) Cell proliferation and morphology analysis of HUVECs seeded on stents*

Likewise, cell viability and morphological analyses were performed for HUVEC-seeded stents. As illustrated in **Figure 6**, compared to stents coated with nanofibers, HUVECs seeded on bare PCL stents showed unfavorable cell adhesion and cell proliferation due to the limited attachment area and the bare surface of PCL struts. As shown in **Figure 6D(i)**, sparse HUVECs adhered to the surface of bare PCL fibers, while RASMCs were spread over PCL fibers (**Figure 5D(i)**). HUVECs seeded on the "Stent + Nano-PDLLA" and "Stent + Nano-PDLLA-DP" groups presented enhanced cell adhesion and proliferation (**Figure 6A** and **6B**) and showed well-spread cellular morphologies (**Figure 6C(ii)**, **6C(iii)**, **6D(ii)**, and **6D(iii)**). The cell proliferation of HUVECs in the "Stent + Nano-PDLLA-DP" group was approximate to that of the "Stent + Nano-PDLLA" group, and the surface of the "Stent + Nano-PDLLA-DP" group was also adequately overspread with HUVECs.

## 3.5. In vivo stent implantation

To further demonstrate that DP-loaded nanofiber-coated stents could alleviate the formation of restenosis, in vivo implantation of stents was carried out. Coronary angiography of the stented artery section was performed to observe the patency of vessels on day 0 and day 28 post-implantation. As shown in **Figure S6**, the angiographic results indicated that arteries implanted with the bare stents showed an obvious reduction in the luminal area compared to arteries implanted with the "Stent + Nano-PDLLA-DP" group. Furthermore, the H&E staining and Masson staining images verified that arteries implanted with bare stents exhibited more severe in-stent restenosis (**Figure 7A-D**). As shown in **Figure 7A** and **7C**, the bare stent group revealed extensive proliferation of SMCs and consequent more serious lumen area loss. Stents

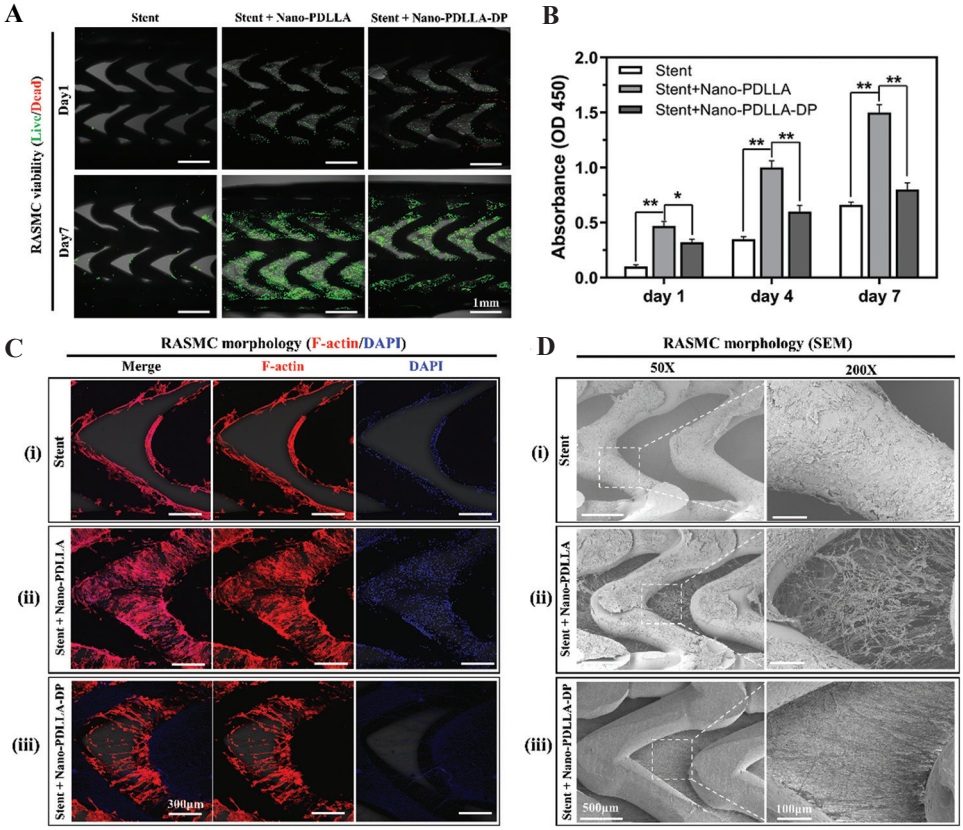


**Figure 5.** Cell proliferation and morphology analysis of RASMCs seeded on different stents. (A) Live/dead staining images of RASMC-seeded stents after culture for 1 day and 7 days. (B) Cell proliferation of RASMCs after seeding on stents for days 1, 4 and 7. (C) F-actin (phalloidin, red) and DAPI (blue) staining of RASMCs after seeding on (C(i)) bare stents, (C(ii)) stents coated with dipyridamole-loaded poly(D,L-lactide) (PDLLA) nanofibers, and (C(iii)) stents coated with PDLLA/DP nanofibers for 7 days. (D) SEM images of RASMCs after seeding on (D(i)) bare stents, (D(ii)) stents coated with PDLLA nanofibers, and (D(iii)) stents coated with PDLLA/DP nanofibers for 7 days. Three samples (n = 3) from each group were used for cell proliferation evaluation. $*P < 0.05$, $**P < 0.01$.

coated with DP-loaded nanofibers significantly reduced the thickness of intimal hyperplasia compared with bare stents, from 506 ± 153 μm to 288 ± 31 μm (**Figure 7E**). Meanwhile, the average neointimal area of stents with DP-loaded coating was decreased by 54% compared to that of the bare stent group, decreasing from 2.14 ± 0.31 $mm^2$ to 0.98 ± 0.15 $mm^2$ (**Figure 7F**). The average neointimal stenosis ratio of stents with DP-loaded coating was remarkably lower (42% vs. 65%) than that of the bare stent group (**Figure 7G**). As shown in **Figure 9**, after implantation for 28 days, CD31 expression around the bare PCL stents was lower than that around the DP-loaded nanofibers coated stents.

## 4. Discussion

Ideally, following the implantation of stents into the arteries, the sustained release of the drug should induce the inhibition of SMC proliferation and allow initial endothelialization with the rapid degradation of the coating polymer material. Subsequently, as the backbone materials slowly degrade, the stent gradually disappears, causing blood vessels to return to a more natural state and recover normal vasomotion[1,3,33]. DP-loaded nanofibers showed the potential for long-term drug release and could prevent SMC proliferation and have no detrimental effect on endothelial cells[21]. Therefore, it is a promising idea to develop a drug-loaded bioresorbable stent by coating 3D-printed biodegradable stents with DP-loaded nanofibers.

To achieve the desired stent degradation and drug elution, polymers with appropriate degradation rates and biocompatibility are essential to act as backbone materials and polymeric coatings. PCL has been widely applied in biomedical applications because of its excellent biocompatibility, flexible printability, suitable mechanical properties, and appropriate degradation rate (24 – 36 months)[34]. PDLLA has been widely used as a drug delivery carrier because of its excellent biocompatibility and suitable degradation rate (9 – 24 months)[35,36]. Hence, PCL and PDLLA were selected to act as the backbone material of the stent and the coating polymer in the present work.

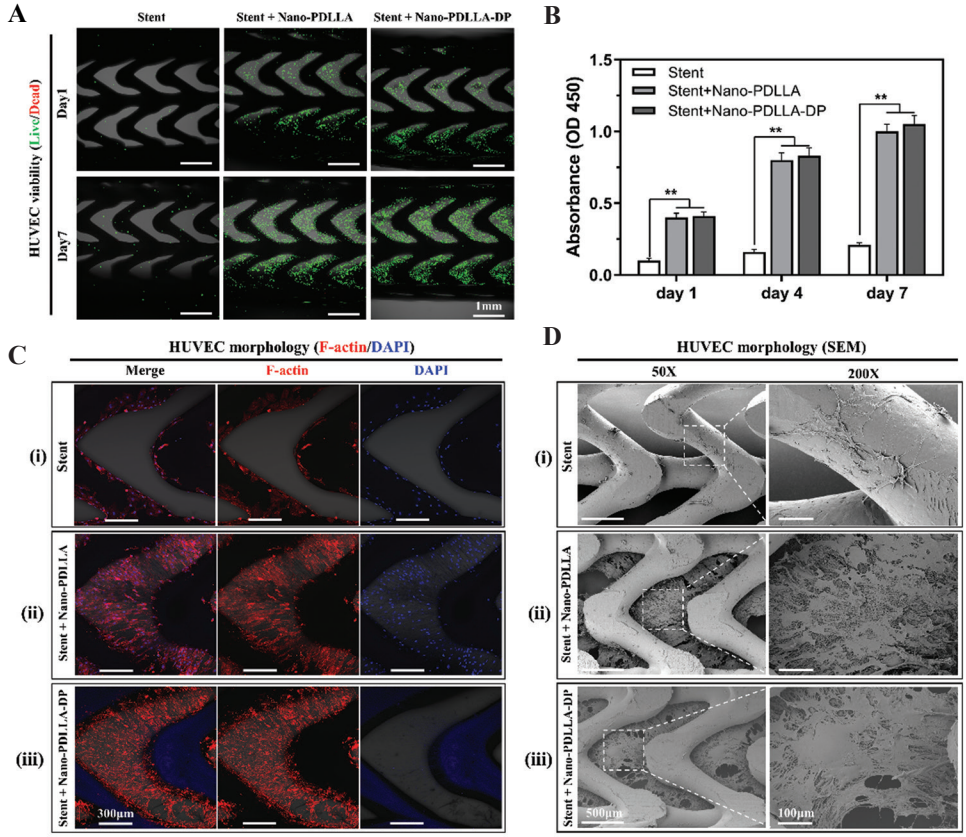


**Figure 6.** Cell proliferation and morphology analysis of HUVECs seeded on different stents. (A) Live/dead staining images of HUVEC-seeded stents after culture for 1 day and 7 days. (B) Cell proliferation of HUVECs after seeding on stents for days 1, 4 and 7. (C) F-actin (phalloidin, red) and DAPI (blue) staining of HUVECs after seeding on (C(i)) bare stents, (C(ii)) stents coated with dipyridamole-loaded poly(D,L-lactide) (PDLLA) nanofibers, and (C(iii)) stents coated with PDLLA/DP nanofibers for 7 days. (D) SEM images of HUVECs after seeding on (D(i)) bare stents, (D(ii)) stents coated with PDLLA nanofibers, and (D(iii)) stents coated with PDLLA/DP nanofibers for 7 days. Three samples (n = 3) from each group were used for cell proliferation evaluation. *$P < 0.05$, **$P < 0.01$.

As shown in **Figure S1** and **Figure 2**, PDLLA/DP nanofibers showed more uniform morphology and reduced average diameter compared to the plain PDLLA nanofibers, which is a result of the differentiation in the solution's electrical conductivity. The electrical conductivity of plain PDLLA/HFIP was 3.64 ± 0.02 μS/cm, while that of solution dissolved with 25 mg/mL of DP was significantly increased to 68.71 ± 0.39 μS/cm. According to the previous works[37], DP molecules added in the polymer solutions exist in an ionic form that could contribute to the electrostatic charge build-up during electrospinning. As the jet exits the tip of the nozzle, it reinforces the effect of the electric field, resulting in thinner fibers. The in vitro drug release and degradation of DP-loaded nanofibers suggested that 120-day long-term sustained release could be achieved accompanied by the degradation of PDLLA fibers. As shown in **Figure 2**, the changes in the distribution and average value of fiber diameter reflected the advancement of fiber degradation. Simultaneously, the drug was continuously released into PBS solution.

Subsequently, we developed 3D-printed PCL stents coated with DP-loaded PDLLA nanofibers, which showed smooth and integral morphology through SEM observation (**Figure 3** and **Figure S3**). Besides, compared to similar stents in the previous studies, stents fabricated in this work exhibited superior radial strength[38,39]. In detail, when the radial deformation was 50%, the stress of the stents in this study was approximately 40 kPa, while that of the stents in the previous studies was approximately 15 kPa. Platelet adhesion and hemolysis tests were performed to assess the hemocompatibility of stents. As presented in **Figure 4**, stents coated with PDLLA nanofibers showed extensively increased platelet adhesion, which was attributed to the introduction of electrospun fibers and the accompanying increasing contact area between the samples and PRP solution. Conversely, the "Stent + Nano-PDLLA-DP" group showed significantly reduced adherent platelets and hemolysis ratio. Hence, the "Stent + Nano-PDLLA-DP" group could prevent platelet adhesion and counteract the adverse effect of increased contact area due to the benefits of DP.

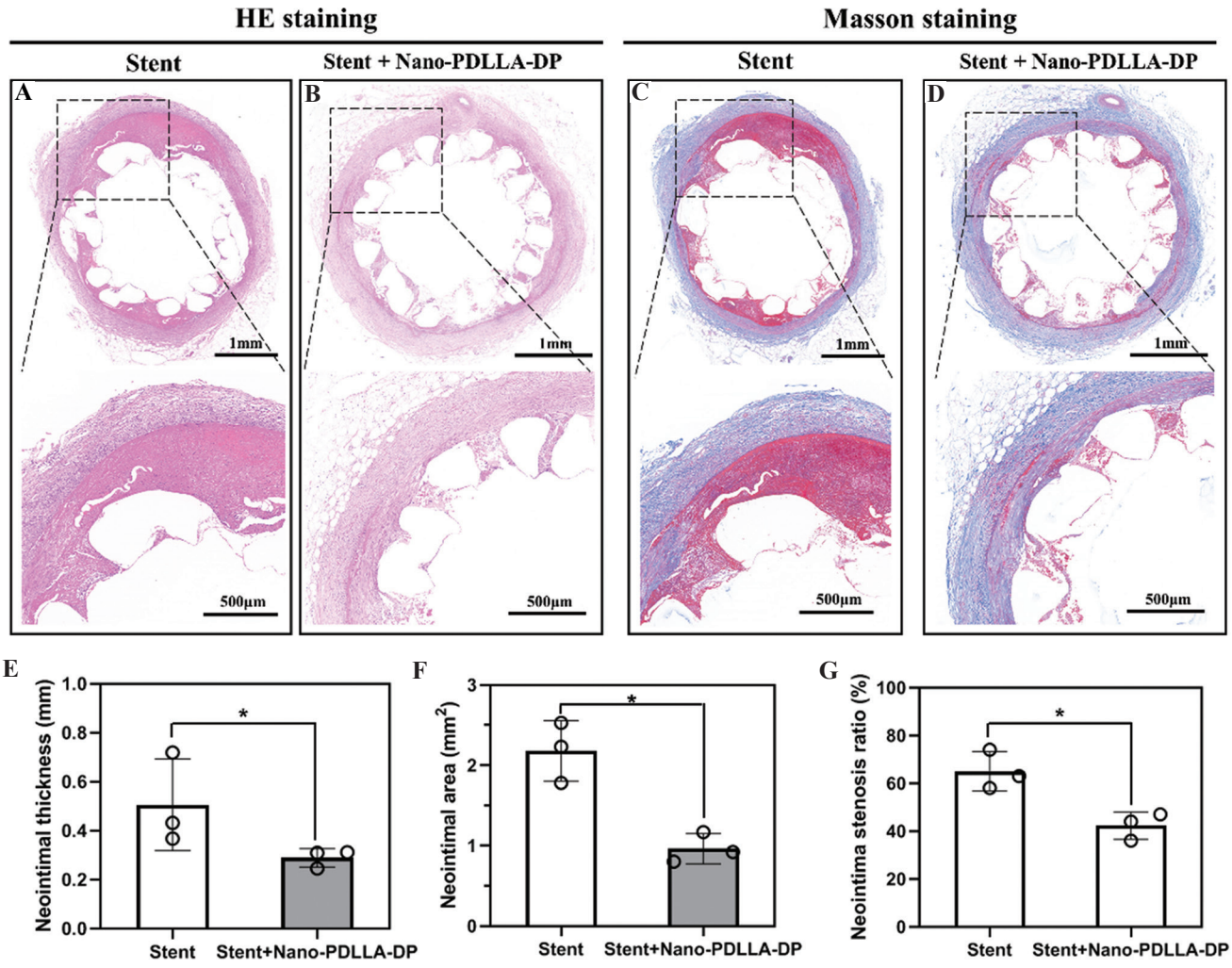


**Figure 7.** In vivo implantation evaluation of the bare stents and stents coated with dipyridamole-loaded poly(D,L-lactide) (PDLLA)/DP nanofibers. H&E staining images of (A) bare stents and (B) stents coated with PDLLA/DP nanofibers. Masson staining images of (C) bare stents and (D) stents coated with PDLLA/DP nanofibers. Quantitative analysis of (C) neointimal thickness, (D) neointimal area, and (E) neointimal stenosis ratio. Three samples (n = 3) from each group were used to analyze neointimal development *$P < 0.05$.

The native arteries consist of three structural layers: intima, media, and adventitia. The intima includes a monolayer of endothelial cells, and the media is composed of abundant vascular SMCs[40]. Adverse reactions after stent implantation are closely related to cellular biological changes in endothelial cells and SMCs. As presented in **Figure S5**, **Figure 5**, and **Figure 6**, both RASMCs and HUVECs seeded on the "Stent + Nano-PDLLA" group showed a significantly higher cell proliferation rate than cells seeded on the bare stents, benefiting from the introduction of nanofibers and an increased contact area for cell attachment and migration. Different cell behaviors of RASMCs and HUVECs were observed in the "Stent + Nano-PDLLA-DP" group. Compared to the "Stent + Nano-PDLLA" group, the cell proliferation of RASMCs seeded on the "Stent + Nano-PDLLA-DP" group showed an obvious decrease due to the continuous release of DP (**Figure 5C(iii)** and **5D(iii)**). In contrast, HUVECs were adequately overspread on the surface of the "Stent + Nano-PDLLA-DP" group, which indicated that the release of DP showed no adverse effects on the cell proliferation and morphology of endothelial cells (**Figure 6C(iii)** and **6D(iii)**). Therefore, it can be determined that 3D-printed stents coated with DP-loaded nanofibers (the "Stent + Nano-PDLLA-DP" group) could obviously prevent the proliferation of SMCs seeded onto stents and have no detrimental effects on the cell viability of endothelial cells.

The in vivo implantation assessment was conducted to further verify the performance of DP-loaded stents. The detriments of stents without drug delivery have been well demonstrated[1-3,8,9]. We believe that PDLLA nanofiber-coated stents without drugs cannot cope with the above-mentioned intimal hyperplasia. Therefore, in this study,

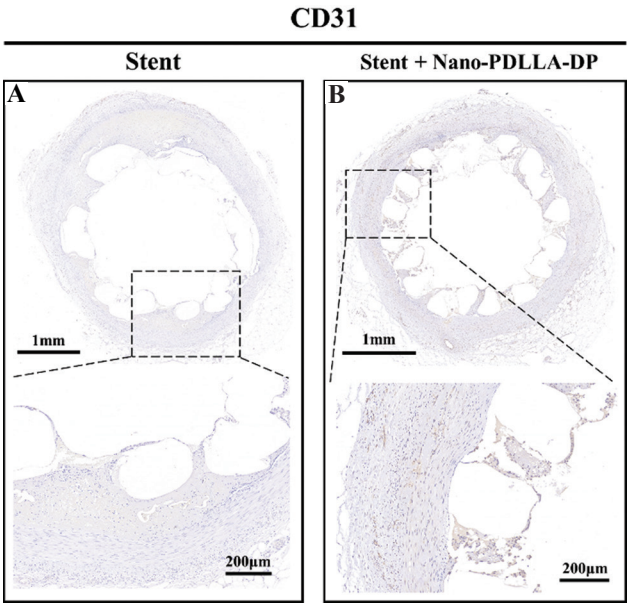


**Figure 8.** Immunohistochemical analysis of the stented arterial segments for CD31 after implantation for 28 days. (A) Bare stents and (B) stents coated with dipyridamole-loaded poly(D,L-lactide)/DP nanofibers.

with the guidance of the 3Rs principle (replace, reduce, and refine), we only retained the "Stent" group as a control group to reduce the number of experimental animals as much as possible. After implantation for 28 days, arteries implanted with DP-loaded stents were observed with a reduction in intimal hyperplasia, the average neointimal area, and the neointimal stenosis ratio (**Figure 7 and Figure S6**). These results suggest that stents coated with DP-loaded nanofibers could effectively inhibit neointimal development. Endothelialization is a hallmark of vascular healing and is important for the prevention of thrombus formation. As presented in **Figure 8**, the neointimal on bare stents showed deficient CD31 expression, indicating the delayed repair of the endothelium. Moreover, continuous initial endothelialization was observed in the inner surface of stents coated with DP-loaded nanofibers, which was a positive signal for long-term vascular patency.

## 5. Conclusions

In this study, we developed an integrated stent with the combination of 3D-printed PCL stents and DP-loaded electrospun nanofibers. Stents coated with nanofibers presented precise structures and possessed enhanced radial strength. The in vitro degradation and drug release evaluation showed a long-term sustained release of DP drug from PDLLA nanofibers over 120 days. With the introduction of DP in fibers, the stents also showed excellent in vitro hemocompatibility. The cell viability and morphological analysis results indicated that stents coated with PDLLA/DP nanofibers could inhibit the proliferation of SMC and had no detrimental effects on endothelial cells in vitro. Furthermore, the in vivo implantation of stents coated with PDLLA/DP nanofibers showed initial patency and continuous endothelialization and alleviated neointimal formation compared to bare stents. Collectively, the integrated stents coated with DP-loaded PDLLA nanofibers showed great potential for restenosis prevention and endothelialization. In future research, the decrease in strut thickness and the long-term in vivo implantation of improved stents will be further explored.

## Acknowledgments

The authors acknowledge funding support from the Tsinghua University Initiative Scientific Research Program (20197050024) and the 111 Project (B17026).

## Conflicts of interest

No conflict of interest was reported by all authors.

## Author contributions

C. W., L. Z., and W. S. proposed the integrated stent design and prepared the manuscript. C. W., Y. Y., and J. J. conducted the experiments. Y. F. and L. O. helped to revise the manuscript. All authors have given approval to the final version of the manuscript.

## References

1. Wiebe J, Nef HM, Hamm CW, 2014, Current Status of Bioresorbable Scaffolds in the Treatment of Coronary Artery Disease. *J Am Coll Cardiol*, 64:2541–51. https://doi.org/10.1016/j.jacc.2014.09.041
2. Wessely R, 2010, New Drug-eluting Stent Concepts. *Nat Rev Cardiol*, 7:194–203. https://doi.org/10.1038/nrcardio.2010.14
3. Ang H Y, Bulluck H, Wong P, *et al.*, 2017, Bioresorbable Stents: Current and Upcoming Bioresorbable Technologies. *Int J Cardiol*, 228:931–9. https://doi.org/10.1016/j.ijcard.2016.11.258
4. Joner M, Finn AV, Farb A, *et al.*, 2006, Pathology of Drug-Eluting Stents in Humans. Delayed Healing and Late Thrombotic Risk. *J Am Coll Cardiol*, 48:193–202. https://doi.org/10.1016/j.jacc.2006.03.042
5. Capranzano P, Dangas G, 2012, Late Stent Thrombosis: The Last Remaining Obstacle in Coronary Interventional Therapy. *Curr Cardiol Rep*, 14:408–17. https://doi.org/10.1007/s11886-012-0283-9
6. Inoue T, Croce K, Morooka T, *et al.*, 2011, Vascular

Inflammation and Repair: Implications for Re-endothelialization, Restenosis, and Stent Thrombosis. *JACC: Cardiovasc Interv*, 4:1057–66. https://doi.org/10.1016/j.jcin.2011.05.025

7. Jinnouchi H, Torii S, Sakamoto A, *et al.*, 2019, Fully bioresorbable vascular scaffolds: lessons learned and future directions. *Nat Rev Cardiol*, 16:286–304. https://doi.org/10.1038/s41569-018-0124-7
8. Onuma Y, Ormiston J, Serruys PW, 2011, Bioresorbable Scaffold Technologies. *Circ J*, 75:509–20. https://doi.org/10.1253/circj.CJ-10-1135
9. Iqbal J, Onuma Y, Ormiston J, *et al.*, 2014, Bioresorbable Scaffolds: Rationale, Current Status, Challenges, and Future. *Eur Heart J*, 35:765–76. https://doi.org/10.1093/eurheartj/eht542
10. Toong DW, Ng JC, Huang Y, *et al.*, 2020, Bioresorbable Metals in Cardiovascular Stents: Material Insights and Progress. *Materialia*, 12:100727. https://doi.org/10.1016/j.mtla.2020.100727
11. Wang C, Zhang L, Fang Y, *et al.*, 2021, Design, Characterization, and 3D Printing of Cardiovascular Stents with Zero Poisson's Ratio in Longitudinal Deformation. *Engineering*, 7:979–90. https://doi.org/10.1016/j.eng.2020.02.013
12. Zhuplatov SB, Masaki T, Blumenthal DK, *et al.*, 2006, Mechanism of Dipyridamole's Action in Inhibition of Venous and Arterial Smooth Muscle Cell Proliferation. *Basic Clin Pharmacol Toxicol*, 99:431–9. https://doi.org/10.1111/j.1742-7843.2006.pto_516.x
13. Mattfeldt T, Mall G, 1983, Dipyridamole-induced Capillary Endothelial Cell Proliferation in the Rat Heart a Morphometric Investigation. *Cardiovasc Res*, 17:229–37. https://doi.org/10.1093/cvr/17.4.229
14. Lamichhane S, Gallo A, Mani G, 2014, A Polymer-free Paclitaxel Eluting Coronary Stent: Effects of Solvents, Drug Concentrations and Coating Methods. *Ann Biomed Eng*, 42:1170–84. https://doi.org/10.1007/s10439-014-1003-y
15. Chen MC, Liang HF, Chiu YL, *et al.*, 2005, A Novel Drug-eluting Stent Spray-coated with Multi-layers of Collagen and Sirolimus. *J Control Release*, 108:178–89. https://doi.org/10.1016/j.jconrel.2005.07.022
16. Huang Y, Subbu SS, Boey FY, *et al.*, 2010, In vitro and In vivo Performance of a Dual Drug-eluting Stent (DDES). *Biomaterials*, 31:4382–91. https://doi.org/10.1016/j.biomaterials.2010.01.147
17. Oh Band Lee CH, 2013, Advanced Cardiovascular Stent Coated with Nanofiber. *Mol Pharm*, 10:4432–42. https://doi.org/10.1021/mp400231p
18. Tan GZ, Zhou Y, 2019, Electrospinning of Biomimetic Fibrous Scaffolds for Tissue Engineering: A Review. *Int J Polym Mater Polym Biomater*, 69:947–60. https://doi.org/10.1080/00914037.2019.1636248
19. Oh B, Lee CH, 2013, Nanofiber for Cardiovascular Tissue Engineering. *Expert Opin Drug Deliv*, 10:1565–82.
20. Hu X, Liu S, Zhou G, *et al.*, 2014, Electrospinning of Polymeric Nanofibers for Drug Delivery Applications. *J Control Release*, 185:12–21. https://doi.org/10.1016/j.jconrel.2014.04.018
21. Punnakitikashem P, Truong D, Menon JU, *et al.*, 2014, Electrospun Biodegradable Elastic Polyurethane Scaffolds with Dipyridamole Release for Small Diameter Vascular Grafts. *Acta Biomater*, 10:4618–28. https://doi.org/10.1016/j.actbio.2014.07.031
22. Liu P, Liu Y, Li P, *et al.*, 2018, Rosuvastatin-and Heparin-Loaded Poly(l-lactide- co-caprolactone) Nanofiber Aneurysm Stent Promotes Endothelialization via Vascular Endothelial Growth Factor Type A Modulation. *ACS Appl Mater Interf*, 10:41012-41018. https://doi.org/10.1021/acsami.8b11714
23. Wang C, Xu Y, Xia J, *et al.*, 2021, Multi-scale Hierarchical Scaffolds with Aligned Micro-fibers for Promoting Cell Alignment. *Biomed Mater* (*Bristol*), 16:ac0a90. https://doi.org/10.1088/1748-605X/ac0a90
24. Lin S, Ran X, Yan X, *et al.*, 2019, Corrosion Behavior and Biocompatibility Evaluation of a Novel Zinc-based Alloy Stent in Rabbit Carotid Artery Model. *J Biomed Mater Res Part B Appl Biomater*, 107:1814–1823. https://doi.org/10.1002/jbm.b.34274
25. Im SH, Kim CY, Jung Y, *et al.*, 2017, Biodegradable Vascular Stents with High Tensile and Compressive Strength: A Novel Strategy for Applying Monofilaments Via Solid-state Drawing and Shaped-annealing Processes. *Biomater Sci*, 5:422–31. https://doi.org/10.1039/c7bm00011a
26. Xue J, Wu T, Dai Y, *et al.*, 2019, Electrospinning and Electrospun Nanofibers: Methods, Materials, and Applications. *Chem Rev*, 119:5298–415. https://doi.org/10.1021/acs.chemrev.8b00593
27. Fong H, Chunand I, Reneker DH, 1999, Beaded Nanofibers Formed during Electrospinning. *Polymer*, 40:4585–92.
28. Qin Y, Liu R, Zhao Y, *et al.*, 2016, Preparation of Dipyridamole/Polyurethane Core-shell Nanofibers by Coaxial Electrospinning for Controlled-release Antiplatelet

Application. *J Nanosci Nanotechnol*, 16:6860–6. https://doi.org/10.1166/jnn.2016.11386

29. Repanas A, Wolkers WF, Gryshkov OP, *et al.*, 2015, Pcl/Peg Electrospun Fibers as Drug Carriers for the Controlled Delivery of Dipyridamole. *J In Silico* In vitro *Pharmacol*, 1:1–10. https://doi.org/10.21767/2469-6692.10003
30. Ruggeri ZM, Mendolicchio GL, 2007, Adhesion Mechanisms in Platelet Function. *Circ Res*, 100:1673–85. https://doi.org/10.1161/01.RES.0000267878.97021.ab
31. Li W, Zhou J, Xu Y, 2015, Study of the In vitro Cytotoxicity Testing of Medical Devices. *Biomed Rep*, 3:617–20. https://doi.org/10.3892/br.2015.481
32. 10993-5:2009 I, Biological Evaluation of Medical Devices Part 5: Tests for In vitro Cytotoxicity. Technical Committee.
33. Wu X, Wu S, Kawashima H, *et al.*, 2021, Current Perspectives on Bioresorbable Scaffolds in Coronary Intervention and other Fields. *Expert Rev Med Dev*, 18:351–65. https://doi.org/10.1080/17434440.2021.1904894
34. Woodruff MA, Hutmacher DW, 2010, The Return of a Forgotten Polymer Polycaprolactone in the 21st Century. *Prog Polym Sci* (*Oxford*), 35:1217–56. https://doi.org/10.1016/j.progpolymsci.2010.04.002
35. Kim K, Yu M, Zong X, *et al.*, 2003, Control of Degradation Rate and Hydrophilicity in Electrospun Non-woven Poly(D,L-lactide) Nanofiber Scaffolds for Biomedical Applications. *Biomaterials*, 24:4977–85. https://doi.org/10.1016/S0142-9612(03)00407-1
36. Ulery BD, Nair LS, Laurencin CT, 2011, Biomedical Applications of Biodegradable Polymers. *J Polym Sci Part B Polym Phys*, 49:832–64. https://doi.org/10.1002/polb.22259
37. Repanas A, Glasmacher B, 2015, Dipyridamole Embedded in Polycaprolactone Fibers Prepared by Coaxial Electrospinning as a Novel Drug Delivery System. *J Drug Deliv Sci Technol*, 29:132–42. https://doi.org/10.1016/j.jddst.2015.07.001
38. Qiu T, Jiang W, Yan P, *et al.*, 2020, Development of 3D-Printed Sulfated Chitosan Modified Bioresorbable Stents for Coronary Artery Disease. *Front Bioeng Biotechnol*, 8:462. https://doi.org/10.3389/fbioe.2020.00462
39. Lei D, Luo B, Guo Y, *et al.*, 2019, 4-Axis Printing Microfibrous Tubular Scaffold and Tracheal Cartilage Application. *Sci China Mater*, 62:1910–20. https://doi.org/10.1007/s40843-019-9498-5
40. Martinez-Lemus LA, 2012, The Dynamic Structure of Arterioles. *Basic Clin Pharmacol Toxicol*, 110:5–11. https://doi.org/10.1111/j.1742-7843.2011.00813.x

## Publisher's note